

ROBERT KOCH INSTITUT



Originally published as:

Woznik, M., Rödner, C., Lemon, K., Rima, B., Mankertz, A., Finsterbusch, T.
Mumps virus small hydrophobic protein targets ataxin-1 ubiquitin-like interacting protein (ubiquilin 4)
(2010) *Journal of General Virology*, 91 (11), pp. 2773-2781.

DOI: 10.1099/vir.0.024638-0

This is an author manuscript that has been accepted for publication in *Journal of General Virology*, copyright Society for General Microbiology, but has not been copy-edited, formatted or proofed. Cite this article as appearing in *Journal of General Virology*. This version of the manuscript may not be duplicated or reproduced, other than for personal use or within the rule of 'Fair Use of Copyrighted Materials' (section 17, Title 17, US Code), without permission from the copyright owner, Society for General Microbiology. The Society for General Microbiology disclaims any responsibility or liability for errors or omissions in this version of the manuscript or in any version derived from it by any other parties. The final copy-edited, published article, which is the version of record, can be found at <http://vir.sgmjournals.org>, and is freely available without a subscription.

Mumps virus small hydrophobic protein targets ataxin-1 ubiquitin-like interacting protein (ubiquilin 4)

Maria Woznik,^{1,2} Claudia Röchner,³ Ken Lemon,⁴ Bert Rima,⁴ Annette Mankertz^{2,†} and Tim Finsterbusch^{2,†}

¹ Department of Biology, Chemistry and Pharmacy, FU-Berlin, Takustra. 3, 14195 Berlin, Germany

² National Reference Centre Measles, Mumps, Rubella, Division of Viral Infections (FG12), Robert Koch Institute, Nordufer 20, 13353 Berlin, Germany

³ Lampe Konieczny & Company GmbH & Co. KG, Gustav-Meyer-Allee 25, 13355 Berlin, Germany

⁴ School of Medicine, Dentistry and Biomedical Sciences, Centre for Infection and Immunity, Queen's University Belfast, 97 Lisburn Road, Belfast BT9 7BL, UK

† These authors contributed equally to this work.

Correspondence: Tim Finsterbusch; finsterbuscht@rki.de

The small hydrophobic (SH) protein of mumps virus has been reported to interfere with innate immunity by inhibiting tumour necrosis factor alpha-mediated apoptosis. In a yeast two-hybrid screen we have identified the ataxin-1 ubiquitin-like interacting protein (A1Up) as a cellular target of the SH protein. A1Up contains an amino-terminal ubiquitin-like (UbL) domain, a carboxyterminal ubiquitin-associated (UbA) domain and two stress-inducible heat shock chaperoninbinding (Sti1) motifs. This places it within the ubiquitin-like protein family that is involved in proteasome-mediated activities. Co-immunoprecipitation confirmed the binding of SH and A1Up and demonstrates that a truncated protein fragment corresponding to aa 136–270 of A1Up, which represents the first Sti1-like repeat and an adjacent hydrophobic region, was sufficient for interaction, whereas neither the UbL nor the UbA domains were required for interaction. The ectopic expression of A1Up leads to a redistribution of SH to punctate structures that co-localize with the 20S proteasome in transfected or infected mammalian cells.

Introduction

Mumps virus (MuV) belongs to the family Paramyxoviridae, genus Rubulavirus. This enveloped virus contains a 15 384 nt non-segmented, ssRNA genome of negative polarity. MuV causes an acute communicable childhood disease characterized by fever and parotitis. The virus is transmitted via the respiratory route and is often disseminated to the CNS (Carbone & Rubin, 2007). Hence, MuV infection was the most common cause of aseptic meningitis prior to vaccination being available for it (Watson et al., 1998).

The SH gene of MuV is highly variable. Consequently, a 316 nt fragment comprising the SH mRNA is used for MuV genotyping. Phylogenetic comparison of the SH gene from virus isolates has led to the definition of 12 MuV genotypes, which have been designated A–L (Jin et al., 2005). Recently a new genotype, M, was described (Santos et al., 2008). The SH (small hydrophobic) protein of MuV is expressed in MuV-infected cells but is not a constituent part of the virion (Takeuchi et al., 1996). SH is apparently non-essential for viral replication in cell culture, since the growth rate of cell culture-adapted strain Enders, which does not express the SH protein, is not restricted compared with wild-type MuV strains (Afzal et al., 1990; Takeuchi et al., 1991). Though the SH proteins of other paramyxoviruses, e.g. human respiratory syncytial virus (HRSV) and parainfluenza virus 5 (PIV5, formerly also named SV5), do not share any sequence homology with the MuV SH protein, all have been reported to be involved in blocking the tumour necrosis factor alpha (TNF- α)-mediated apoptosis pathway by inhibition of TNF- α signalling. Furthermore, a recombinant PIV5, in which the original SH has been

replaced by that of HRSV or MuV, was able to block TNF- α -induced apoptosis (Fuentes et al., 2007; Wilson et al., 2006). In addition, the SH protein of HRSV has been predicted to act as a viroporin (Perez et al., 1997; Kochva et al., 2003). Viroporins are a group of highly hydrophobic small viral proteins that are able to homo-oligomerize and induce membrane permeability (Gonzalez & Carrasco, 2003).

The ataxin-1 ubiquitin-like interacting protein (A1Up), also known as ubiquilin 4, is involved in proteasome-mediated degradation of proteins and interacts with ataxin-1, a protein associated with the neurodegenerative disease spinocerebellar ataxia type 1 (Davidson et al., 2000). A1Up contains several protein motifs characteristic for ubiquilin proteins. These include an amino-terminal ubiquitin-like (UBL) domain that is responsible for binding to the S5a subunit of the 19S proteasome (Hiyama et al., 1999) and a carboxy-terminal ubiquitin associated UbA domain that interacts with polyubiquitinated proteins and thereby initiates their proteasome-mediated degradation (Riley et al., 2004). A1Up also contains two stress-inducible heat shock chaperonin binding (Sti1) motifs that are known to bind to a wide range of cellular proteins. The first Sti1 motif of A1Up has been reported to bind to proteins with endoplasmic reticulum (ER) signal sequences. It is preceded by a hydrophobic region that enhances binding by attaching A1Up to the ER membrane via hydrophobic interactions (Matsuda et al., 2001).

The role of the SH protein of MuV in the process of MuV infection is still largely unknown. For this study, we investigated the field of virus–host cell interaction to gain more detailed knowledge about the function of the SH protein. We determined early in this study that A1Up is a cellular interaction partner and we concentrated on this.

Results

Cellular proteins binding to SH

To identify cellular proteins interacting with the SH protein of MuV, the SH protein of the vaccine strain Jeryl Lynn 2 (SH_{JL}) was used as bait in a yeast two-hybrid screen. Six million independent clones from a human cDNA library were screened for interaction with the SH protein. A total of 17 positive clones were rescued, sequenced and analysed by BLAST search. Similarity to three human proteins was found. Three clones matched the carboxy-terminal region of A1Up (601 aa; GenBank accession no. NP_064516), with the largest fragment (A1U₀) showing 99% identity with the last 426 aa. One clone (GPR125₀) showed 99% identity to the carboxyterminal 379 aa of human G protein-coupled receptor 125 (GPR125, 1312 aa; GenBank accession no. NP_660333). Three clones corresponded to the human renin receptor (RR, 350 aa; GenBank accession no. NP_005756); clone RR₀ was 100% identical to the carboxy-terminal 250 aa of the human RR. The remaining ten clones did not encode ORFs with marked similarity to known proteins. In the following we will focus on the interaction of SH and A1Up. The interaction of SH with the receptor proteins GPR125 and RR will be described elsewhere. A1U₀ was retested for interaction by co-transformation with vector pGBKT7 or with the bait construct pBD–SH_{JL} into yeast strain AH109 (Fig. 1a). Co-transformation was confirmed by growth on double drop-out (DDO) plates (Fig. 1a, lower panel), while growth of blue colonies on quadruple drop-out plates containing X- α -Gal (QDO/X) plates implied interaction of the two proteins. When A1U₀, RR₀ and GPR125₀ were tested for interaction with a wild-type MuV SH protein (SH_{wt}), by yeast two hybrid screening, interaction was similarly observed (data not shown).

Co-immunoprecipitation of SH and A1Up

The physical interaction of both SH_{wt} and SH_{JL} with A1Up was confirmed by co-immunoprecipitation (co-IP). Haemagglutinin (HA)-tagged SH (pHA–SH_{wt}) was coexpressed with Myc-tagged full-length A1Up (pMyc– A1Up) in 293 cells. The cells were lysed and incubated with rabbit anti-HA antiserum. The protein complexes were precipitated with protein G–Sepharose, separated by SDS-PAGE and analysed by immunoblotting. A1Up coprecipitated with the SH protein (Fig. 1b, lane 1). As negative controls, A1Up was either co-expressed with SH and then incubated with non-specific rabbit IgG (lane 2) or solely expressed and then incubated with rabbit anti-HA (lane 3). Both negative controls showed no significant degree of co-precipitation; the faint band appearing in the latter case is presumably due to non-specific precipitation. Co-IP with SH_{JL} led to identical results (data not shown).

Mapping the domains of A1Up for interaction with SH

As a ubiquitin, A1Up contains an amino-terminal UbL domain, a carboxy-terminal UbA domain and two Sti1 motifs. A hydrophobic region precedes the first Sti1 motif. To investigate whether these elements are required for the interaction with SH, several truncated A1Up versions were constructed (Fig. 2a) and subjected to co-IP assays with the SH protein. A1Up fragments lacking the UbA domain (expressed by pMyc- Δ_{UbA}), the UbL domain and the hydrophobic region (expressed by pMyc-A1U₀) or both the UbA and UbL domains (expressed by pMyc-pMyc-A1U_{DUbL/A}) co-precipitated with the SH protein (Fig. 2b, lanes 1a, 2a and 3a), implying that neither the UbL nor the UbA domain is necessary for binding SH. To investigate the role of the Sti1 motifs in the interaction with SH, truncated fragments of A1Up containing the Sti1 motifs in various combinations were tested. Fragment A1U₁₃₆₋₂₇₀, comprising the first Sti1 motif and the hydrophobic region, interacted with SH (Fig. 2b, lane 5a), while A1U₁₈₆₋₂₇₀, lacking the hydrophobic region and the amino-terminal fragment A_{1U1-143} did not (Fig. 2b, lanes 4a and 6a). A1U₂₅₉₋₆₀₁, a larger fragment comprising the second Sti1 motif, exhibited a faint signal (Fig. 2b, lane 7a). None of the proteins tested was precipitated in the presence of non-specific rabbit IgG (Fig. 2b, lanes 1b-7b), which was used as the negative control. These results suggest that the interaction of A1Up and SH is not mediated by the UbL and UbA domains. Interaction occurred when either two Sti1 regions or the first Sti1 domain and the hydrophobic region were present. The hydrophobic region might be able to enhance the binding activity of the Sti1 region. A similar effect has been described for the interaction of UBIN, the murine A1Up homologue, and Hsp47 (Matsuda et al., 2001). The weak interaction observed for A1U₂₅₉₋₆₀₁, which contains only the second Sti1 motif, in contrast to A1U₁₈₆₋₂₇₀, which did not show any interacting capacity, might be due merely to the extension of the fragment to a size that allows correct folding of the protein.

Subcellular localization of A1Up and SH

To investigate whether SH and A1Up mutually affect their subcellular localization, 293 cells were transfected with pMyc-A1Up and pHA-SH_{wt} and analysed by confocal laser scanning microscopy. We observed that A1Up formed a punctate pattern within the nucleus and the cytoplasm, as was reported by Davidson et al. (2000), and that the 20S proteasome co-localized with A1Up in these structures (Riley et al., 2004) (Fig. 3a). In cells transfected with SH alone, the proteasome showed an even distribution throughout the cell (Fig. 3b) as in non-transfected cells. Staining against protein disulfide isomerase (PDI) demonstrated that the SH protein was localized in the ER (Fig. 3b), as reported previously by Takeuchi et al. (1996). When pHA-SH_{wt} and pMyc-A1Up were co-expressed, SH was partially redistributed to co-localize with A1Up and the 20S proteasome in the aforementioned punctuate structures (Fig. 3c), which did not co-localize with the ER marker PDI (Fig. 3d). These results demonstrate that A1Up transports the SH protein of MuV to the proteasome. When these experiments were performed with SH_{JL}, the results did not deviate from this (data not shown). To rule out that this effect is related to the ectopic expression of SH, we have investigated the subcellular localization of SH and A1Up in MuV-infected cells (Fig. 4). Vero cells were infected with rMuV EGFP-SH and subsequently transfected with pMyc-A1Up. The EGFP-SH fusion protein expressed by the recombinant virus co-localized with PDI (Fig. 4a) and showed a distribution similar to the ectopically expressed SH in 293 cells. Co-expression with A1Up resulted in redistribution of EGFP-SH to the punctiform structures harbouring A1Up and the proteasome (Fig. 4b). This demonstrates that the interaction of SH and A1Up and the transport of SH to the proteasome are also observed in the context of an MuV infection.

Stability of SH and A1Up

The proteasome is a cellular compartment involved in protein degradation. To study whether the formation of the complex of SH and A1Up and its subsequent transport to the proteasome results in the degradation of SH, pHA-SH_{wt} and pMyc-A1Up were co-transfected into 293 cells. The plasmids were co-transfected with pCMV-HA and pCMV-Myc, respectively, to serve as negative controls. After 48 h, cycloheximide was added to shut down protein synthesis. The amount of SH in the presence or absence of A1Up was compared at different times following cycloheximide treatment. In a reciprocal experiment, the stability of A1Up in the presence of SH was determined. Neither the degradation rate of the SH protein, nor the stability of A1Up, was affected significantly by the presence of their interaction partner (Fig. 5). This experiment was also performed with SH_{JL} and gave similar results (data not shown).

Discussion

In this study we have identified A1Up as a cellular target of the SH protein of MuV. The interaction was demonstrated using yeast two-hybrid and co-IP studies. Moreover, the partial redistribution of SH from the ER to the proteasome after co-expression with A1Up provided additional evidence that both proteins interact specifically. Observations of binding and subcellular redistribution of SH were equal for the SH protein of the live attenuated vaccine Jeryl Lynn and for that of a wild-type MuV of genotype G, indicating that the attenuation of the MuV vaccine strain did not affect the capacity of SH to interact with A1Up.

Since the original parent wild-type viruses are lost, and are thus not available for sequencing, they cannot be compared with current vaccines. Therefore, knowledge about the genetic changes responsible for the loss of virulence is rather scant. Sequence deviations have been described with respect to virulence (Yates et al., 1996) and neurovirulence (Rubin et al., 2003; Lemon et al., 2007), but a genetic marker for attenuation has not yet been defined. Here, we have compared the SH protein of a wild-type MuV and a vaccine. The SH gene is the most variable part of the MuV genome; the sequences of SH_{wt} and SH_{JL} differ by 11 aa (19 %). In this study, no differences with respect to interaction and cellular localization were observed, suggesting that attenuation of MuV does not interfere with the interaction with A1Up. A1Up is one of four highly conserved human ubiquitin proteins. Ubiquitins contain a UbL domain that mediates their interaction with the 19S subunit of the proteasome, a UbA domain that feeds proteins into the ubiquitin–proteasome pathway and two Sti1 motifs. When co-expressed with A1Up, SH was redistributed to the cytoplasm to co-localize with A1Up and the proteasome. This observation suggested that A1Up might bind SH via the UbA domain and thus eventually effectuate an increased degradation rate of the SH protein. We eliminated this suggestion by demonstrating that the capacity of A1Up to bind SH is independent of the presence of the UbA domain, and that furthermore the interaction partners do not mutually influence their degradation rate. This suggests other implications for the SH–A1Up interaction.

Using truncated versions of A1Up we were able to narrow down the location of the interacting domain to the first Sti1 motif and the preceding hydrophobic region. In the case of UBIN, a murine homologue of A1Up, the corresponding region is responsible for the interaction with the ER-targeting signal sequence of Hsp47 (Matsuda et al., 2001). Hsp47, an ER-resident stress-inducible glycoprotein, functions as a collagen-specific molecular chaperone (Nagata, 1996). For human ubiquitin 1 and 2, it was shown that the carboxy-terminal Sti1 motif binds to the ATPase domain of the Hsp70-like Stch protein (Kaye et al., 2000). Bag-1, another Sti1-like-repeat-containing protein, interacts with Hsp70 and thereby inhibits the chaperone activity of Hsp70 (Takayama et al., 1997). Hsp70 modulates NF- κ B signalling pathways in the apoptotic cascade and also acts as an inhibitor of apoptosis at multiple levels, e.g. inhibition of the activation of initiator caspases and inhibition of Bax translocation to the mitochondria (Arya et al., 2007). The MuV SH protein might fit into this picture as a regulator of a potential interaction between A1Up and Hsp70. Moreover, the binding of SH to A1Up could stabilize A1Up in its putatively active monomeric form by occupying the central region of the protein. This part of the protein mediates the formation of protein dimers, which was previously shown for ubiquitin 1 and 2 (Ford & Monteiro, 2006). K7, another small hydrophobic protein encoded by Kaposi's sarcoma-associated herpesvirus (HHV8) that protects cells from apoptosis, interacts with ubiquitin 1. K7 inhibits ubiquitin 1 from binding to and thereby stabilizing I κ B, a regulator of the NF- κ B signalling pathway, which eventually results in the rapid degradation of I κ B and p53 (Feng et al., 2004). We found that the MuV SH protein interacts with ubiquitin 1 as well (data not shown). This might suggest that, for both A1Up and ubiquitin 1, binding to SH interferes with their usual cellular function. Moreover, this may contribute to the dysregulation of the TNF- α -mediated apoptosis pathway, resulting in an anti-apoptotic function. Many viral proteins use several of a wide range of cellular targets to subvert the apoptotic process. The K7 protein of HHV8, for instance, interferes with a number of apoptotic pathways: apart from modulating NF- κ B signalling as mentioned above, it also activates the calcium-modulating cyclophilin ligand, which results in an increase in the cytosolic Ca²⁺ concentration (Feng et al., 2002). Furthermore, K7 binds to Bcl-2 and caspase 3, thus inhibiting caspase activity (Wang et al., 2002). A main feature of paramyxovirus SH proteins is their capacity to inhibit the TNF- α -mediated apoptosis pathway. Beyond that property, the SH protein of HRSV has been reported to act as an ion channel-forming viroporin as well (Kochva et al., 2003; Perez et al., 1997). Some viroporins have the capacity to suppress the induction of apoptosis by manipulating intracellular Ca²⁺ homeostasis, as has been described for the 2B protein of coxsackievirus (Campanella et al., 2004). The molecular mechanisms underlying the MuV SH protein's interference with cellular pathways to prevent the induction of apoptosis, and the role that A1Up plays in this context, remain to be investigated in more

detail. Also to be investigated are the involvement of GPR125 and RR, which were not explored in this study.

In summary, our results revealed new functional aspects of the SH protein, linking it to the proteasome-mediated degradation machinery and to chaperone activities, which might be modulated during MuV infection.

Methods

Cell culture, viruses and plasmids. 293 and Vero cells were grown in Dulbecco's modified Eagle's medium supplemented with 5% (v/v) FCS at 37 °C and 5% CO₂. MuV vaccine strain Jeryl Lynn (Afzal et al., 1993) and wild-type strain 05-063 (isolated in 2005 at the National Reference Centre Measles, Mumps, Rubella) were cultivated in Vero cells. Viral RNA was extracted using a QIAamp Viral RNA Mini Kit (Qiagen) and synthesis of cDNA was performed with MMLV-reverse transcriptase (RT) (Invitrogen) and primer Mu21F (Supplementary Table S1; available in JGV Online). DNA fragments were amplified with restriction site-tagged primers (Supplementary Table S1) and PCR products were inserted via restriction sites which were introduced into the plasmids using standard techniques (Sambrook & Russell, 2001). The MuV vaccine Jeryl Lynn is composed of two substrains, JL2 and JL5, present in a 1 : 5 ratio (Afzal et al., 1993). The SH gene of JL2 (SH_{JL}) was amplified with primers MuSH22F and MuSH23R and cloned into pGBKT7 (Clontech) to obtain construct pBD-SH_{JL}. For construction of pHA-SH_{JL}, SH_{JL} was amplified with primers MuSH22F and MuSH36R and inserted into pCMV-HA (Clontech). SH_{wt} was amplified with primers MuSH71F and MuSH72R and cloned into pGBKT7 and pCMV-HA to obtain plasmids pBD-SH_{wt} and pHA-SH_{wt}. The cDNA library plasmid pACT-A1U₀ was subcloned into pCMV-Myc (Clontech) to produce pMyc-A1U₀. A full-length cDNA clone of A1Up (BC081403) was purchased (RZPD; Imagenes) and used as a template for the amplification of PCR products cloned into pCMV-Myc. The resultant plasmids and the primer pairs employed were: pMyc-A1Up, Mu206F and Mu68R; pMyc-A1U_{ΔUbA}, Mu206F and 3050; pMyc-A1U_{ΔUbL}, 3049 and Mu68R; pMyc-A1U_{ΔUbL/A}, 3049 and 3050; pMyc-¹³⁶⁻²⁷⁰, 3088 and 3091; pMyc-A1U₁₈₆₋₂₇₀, 3089 and 3091; pMyc-A1U₂₅₉₋₆₀₁, 3090 and Mu68R; and pMyc-A1U₁₋₁₄₃, Mu206F and 3093.

Generation of recombinant MuV from cDNA.

The SH gene of the vaccine strain JL5 was amplified from the plasmid pMuV(MPBS) (Lemon et al., 2007) using primers EGFP-SH+ and Mu7307R (Supplementary Table S1). The EGFP gene was amplified from plasmid pEGFP-N1 (Clontech) using primers EGFP-SHF and EGFP-SH (Supplementary Table S1). Overlap extension PCR was used to join the two PCR fragments. The resulting product contained the EGFP ORF fused to the SH ORF via a 5 aa linker (GAGQG). This was cloned into pMuV(MPBS) using the unique BtrI and SgfI restriction sites to generate pMuV-EGFP-SH. A549 cells were infected with MVA-T7 at an m.o.i. of 0.5 and transfected with pMuV-EGFP-SH along with plasmids encoding MuV N, P and L as described previously (Lemon et al., 2007). Extensive CPE was observed following the addition of Vero cells to the transfected monolayers. Plaque-purified virus was passaged three times on Vero cells.

Yeast two-hybrid library screen.

The Matchmaker Gal4 Two-Hybrid System 3 (Clontech) was applied according to the manufacturer's instructions. Yeast strain AH109 (Clontech) was transformed simultaneously with bait (pBD-SH_{JL}) and prey (cDNA library derived from human liver; Clontech) plasmids. Transformed cells were selected on QDO plates lacking adenine, histidine, tryptophan and leucine. Yeast colonies were replated on QDO/X plates containing X-a-Gal (Biosynth) to test for α-galactosidase expression. Blue colonies were subcultured on QDO/X plates to rescue additional library plasmids and to eliminate false positives. For plasmid isolation from yeast cells, colonies were grown in DDO medium (lacking leucine and tryptophan) at 30 °C and 200 r.p.m. for 48 h. (Innova 4430; New Brunswick Scientific) After precipitation, cells were resuspended in 10 μl lyticase (5 U ml⁻¹; Sigma-Aldrich) and incubated for 1 h at 37 °C and 250 r.p.m. (Innova 4430; New Brunswick Scientific) Ten microlitres of 20% SDS was added and plasmids were extracted after a freeze-thaw cycle using a DNA Mini Kit (Qiagen). Escherichia coli DH5α cells were transformed with the DNA samples and prey plasmids were extracted and sequenced. A BLAST analysis was performed using the NCBI BLASTP program.

Immunoprecipitation and immunoblot analysis.

293 cells were grown in six-well plates and transfected simultaneously with 200 ng plasmid DNA of pCMV–Myc-based constructs expressing full-length or truncated versions of A1Up and 200 ng of pHA–SH_{wt} or pCMV–HA, using Effectene transfection reagent (Qiagen). Forty-eight hours post-transfection, cells were washed with PBS (pH 7.2) and incubated on ice for 1 h in 1 ml lysis buffer [150 mM NaCl, 5 mM MgCl₂, 20 mM Tris/HCl pH 8, 1 mM EDTA, 1% IGEPAL (Rhodia)] containing one tablet complete mini protease inhibitor per 20 ml (Roche Diagnostics). After the addition of rabbit anti-HA antibody (Hiss Diagnostics) or non-specific rabbit IgG (Dianova), samples were incubated for 2 h at 4 °C. Then 20 µl of protein G–Sepharose was added, followed by incubation for 2 h at 4 °C. The adsorbates were washed four times in PBS (pH 7.2) with 0.2% IGEPAL and subjected to SDS-PAGE (11% acrylamide). Aliquots of complete cell lysates (50 µl) were included as input controls. Proteins were electrophoretically transferred to a PVDF membrane (Millipore). The membranes were blocked with 5% milk powder in PBS (pH 7.2) and 0.05% Tween 20 (PBS-T), and probed with monoclonal anti-HA, anti-Myc or anti-β-actin antibodies (Sigma). The membranes were washed and incubated with HRP-conjugated goat anti-mouse antiserum (Dianova). The antigen– antibody complexes were visualized by chemiluminescence using an ECL–Western blotting detection system (Amersham).

Immunofluorescence analysis.

293 cells were grown on coverslips in 24-well plates. For each transfection, a total of 200 ng plasmid DNA was used. Cells were either simultaneously transfected with pHA–SH_{wt} and pMyc–A1Up or were singly transfected. Twenty-four hours after transfection, cells were fixed with 4% paraformaldehyde in PBS (pH 7.2) and permeabilized with 0.1% Triton X-100 in PBS (pH 7.2). The primary antibodies were labelled with the respective Fab conjugates in separate reactions. The antibody and the respective Fab fragment were mixed, incubated for 20 min at room temperature and then non-bound Fab conjugates were captured by adding a large excess of non-specific mouse, rabbit or goat IgG (Dianova) and incubating for 15 min at room temperature. The labelled antibodies were then diluted in blocking solution and added to the cells for 1 h. HA- or Myc-tagged proteins were detected with monoclonal anti-HA or anti-Myc antibodies (Sigma). ER staining was performed with monoclonal anti-PDI antibody (Acris Antibodies) and the proteasome was detected with rabbit anti-20S proteasome antiserum (Biomol). Cells were washed and nuclei were stained with DAPI (Roth) in PBS-T with 2% BSA for 5 min. Coverslips were mounted in Mowiol (Merck Biosciences) and analysed by confocal laser scanning microscopy (LSM 510; Zeiss). Visualization of DAPI was performed at 355 nm, Cy2-labelled proteins were detected at 488 nm, Cy3-labelled proteins at 594 nm and Cy5-labelled proteins at 688 nm.

Degradation rates of SH and A1Up.

293 cells were grown in sixwell plates and co-transfected with 200 ng pHA–SH_{wt} and pCMV– Myc or pHA–SH_{wt} and pMyc–A1Up, using the Effectene transfection reagent (Qiagen). Twenty-four hours after transfection, cells were split 1 : 10 into 96-well plates and incubated with 50 ng cycloheximide ml⁻¹ (Sigma) for the indicated time (see Fig. 5), followed by fixation with a 1 : 1 solution of methanol/acetone for 15 min at 220 °C. Cells were blocked for 1 h in PBS-T containing 2% milk powder and incubated for 1 h with monoclonal anti-Myc or anti-HA antibody (Sigma). After five washing steps, cells were incubated for 45 min with HRP-conjugated goat anti-mouse antiserum (Dianova) in blocking buffer. Fifty microlitres of 3,3',5,5'-tetramethylbenzidine substrate per well was added and after 20 min the reaction was stopped with an equal amount of 1M H₂SO₄. Reaction intensity was measured at 450 nm with 620 nm as the reference using an ELISA reader (FLUOstar Omega; BMG Labtech).

Acknowledgements

The authors thank Anne Wolbert for valuable discussion and manuscript preparation and Petra Kurzendörfer for excellent technical assistance.

References

- Afzal, M. A., Elliott, G. D., Rima, B. K. & Orvell, C. (1990).** Virus and host cell-dependent variation in transcription of the mumps virus genome. *J Gen Virol* 71, 615–619.
- Afzal, M. A., Pickford, A. R., Forsey, T., Heath, A. B. & Minor, P. D. (1993).** The Jeryl Lynn vaccine strain of mumps virus is a mixture of two distinct isolates. *J Gen Virol* 74, 917–920.
- Arya, R., Mallik, M. & Lakhota, S. C. (2007).** Heat shock genes –integrating cell survival and death. *J Biosci* 32, 595–610.
- Campanella, M., de Jong, A. S., Lanke, K. W., Melchers, W. J., Willems, P. H., Pinton, P., Rizzuto, R. & van Kuppeveld, F. J. (2004).** The coxsackievirus 2B protein suppresses apoptotic host cell responses by manipulating intracellular Ca²⁺ homeostasis. *J Biol Chem* 279, 18440–18450.
- Carbone, K. & Rubin, S. A. (2007).** *Paramyxoviridae: mumps virus*. In *Fields Virology*, 5th edn, pp. 1527–1550. Edited by D. M. Knipe. & P. M. Howley. Baltimore, MD: Williams & Wilkins.
- Davidson, J. D., Riley, B., Burright, E. N., Duvick, L. A., Zoghbi, H. Y. & Orr, H. T. (2000).** Identification and characterization of an ataxin-1- interacting protein: A1Up, a ubiquitin-like nuclear protein. *Hum Mol Genet* 9, 2305–2312.
- Feng, P., Park, J., Lee, B. S., Lee, S. H., Bram, R. J. & Jung, J. U. (2002).** Kaposi's sarcoma-associated herpesvirus mitochondrial K7 protein targets a cellular calcium-modulating cyclophilin ligand to modulate intracellular calcium concentration and inhibit apoptosis. *J Virol* 76, 11491–11504.
- Feng, P., Scott, C. W., Cho, N. H., Nakamura, H., Chung, Y. H., Monteiro, M. J. & Jung, J. U. (2004).** Kaposi's sarcoma-associated herpesvirus K7 protein targets a ubiquitin-like/ubiquitin-associated domain-containing protein to promote protein degradation. *Mol Cell Biol* 24, 3938–3948.
- Ford, D. L. & Monteiro, M. J. (2006).** Dimerization of ubiquilin is dependent upon the central region of the protein: evidence that the monomer, but not the dimer, is involved in binding presenilins. *Biochem J* 399, 397–404.
- Fuentes, S., Tran, K. C., Luthra, P., Teng, M. N. & He, B. (2007).** Function of the respiratory syncytial virus small hydrophobic protein. *J Virol* 81, 8361–8366.
- Gonzalez, M. E. & Carrasco, L. (2003).** Viroporins. *FEBS Lett* 552, 28–34.
- Hiyama, H., Yokoi, M., Masutani, C., Sugawara, K., Maekawa, T., Tanaka, K., Hoeijmakers, J. H. & Hanaoka, F. (1999).** Interaction of hHR23 with S5a. The ubiquitin-like domain of hHR23 mediates interaction with S5a subunit of 26 S proteasome. *J Biol Chem* 274, 28019–28025.
- Jin, L., Rima, B., Brown, D., Orvell, C., Tecle, T., Afzal, M., Uchida, K., Nakayama, T., Song, J. W. & other authors (2005).** Proposal for genetic characterisation of wild-type mumps strains: preliminary standardisation of the nomenclature. *Arch Virol* 150, 1903–1909.
- Kaye, F. J., Modi, S., Ivanovska, I., Koonin, E. V., Thress, K., Kubo, A., Kornbluth, S. & Rose, M. D. (2000).** A family of ubiquitin-like proteins binds the ATPase domain of Hsp70-like Stch. *FEBS Lett* 467, 348–355.
- Kochva, U., Leonov, H. & Arkin, I. T. (2003).** Modeling the structure of the respiratory syncytial virus small hydrophobic protein by silent mutation analysis of global searching molecular dynamics. *Protein Sci* 12, 2668–2674.
- Lemon, K., Rima, B. K., McQuaid, S., Allen, I. V. & Duprex, W. P. (2007).** The F gene of rodent brain-adapted mumps virus is a major determinant of neurovirulence. *J Virol* 81, 8293–8302.
- Matsuda, M., Koide, T., Yoriuzzi, T., Hosokawa, N. & Nagata, K. (2001).** Molecular cloning of a novel ubiquitin-like protein, UBIN, that binds to ER targeting signal sequences. *Biochem Biophys Res Commun* 280, 535–540.
- Nagata, K. (1996).** Hsp47: a collagen-specific molecular chaperone. *Trends Biochem Sci* 21, 22–26.
- Perez, M., Garcia-Barreno, B., Melero, J. A., Carrasco, L. & Guinea, R. (1997).** Membrane permeability changes induced in *Escherichia coli* by the SH protein of human respiratory syncytial virus. *Virology* 235, 342–351.
- Riley, B. E., Xu, Y., Zoghbi, H. Y. & Orr, H. T. (2004).** The effects of the polyglutamine repeat protein ataxin-1 on the Ubl-UBA protein A1Up. *J Biol Chem* 279, 42290–42301.
- Rubin, S. A., Amexis, G., Pletnikov, M., Li, Z., Vanderzanden, J., Mauldin, J., Sauder, C., Malik, T., Chumakov, K. & Carbone, K. M. (2003).** Changes in mumps virus gene sequence associated with variability in neurovirulent phenotype. *J Virol* 77, 11616–11624.

Sambrook, J. & Russell, D. W. (2001). Molecular Cloning: a Laboratory Manual. Cold Spring Harbor, NY: Cold Spring Harbor Laboratory.

Santos, C. L., Ishida, M. A., Foster, P. G., Sallum, M. A., Benega, M. A., Borges, D. B., Correa, K. O., Constantino, C. R., Afzal, M. A. & Paiva, T. M. (2008). Detection of a new mumps virus genotype during parotitis epidemic of 2006–2007 in the state of Sao Paulo, Brazil. *J Med Virol* 80, 323–329.

Takayama, S., Bimston, D. N., Matsuzawa, S., Freeman, B. C., Aime-Sempe, C., Xie, Z., Morimoto, R. I. & Reed, J. C. (1997). BAG-1 modulates the chaperone activity of Hsp70/Hsc70. *EMBO J* 16, 4887–4896.

Takeuchi, K., Tanabayashi, K., Hishiyama, M., Yamada, A. & Sugiura, A. (1991). Variations of nucleotide sequences and transcription of the SH gene among mumps virus strains. *Virology* 181, 364–366.

Takeuchi, K., Tanabayashi, K., Hishiyama, M. & Yamada, A. (1996). The mumps virus SH protein is a membrane protein and not essential for virus growth. *Virology* 225, 156–162.

Wang, H. W., Sharp, T. V., Koumi, A., Koentges, G. & Boshoff, C. (2002). Characterization of an anti-apoptotic glycoprotein encoded by Kaposi's sarcoma-associated herpesvirus which resembles a spliced variant of human survivin. *EMBO J* 21, 2602–2615.

Watson, J. C., Hadler, S. C., Dykewicz, C. A., Reef, S. & Phillips, L. (1998). Measles, mumps, and rubella – vaccine use and strategies for elimination of measles, rubella, and congenital rubella syndrome and control of mumps: recommendations of the Advisory Committee on Immunization Practices (ACIP). *MMWR Recomm Rep* 47 (RR-8), 1–57.

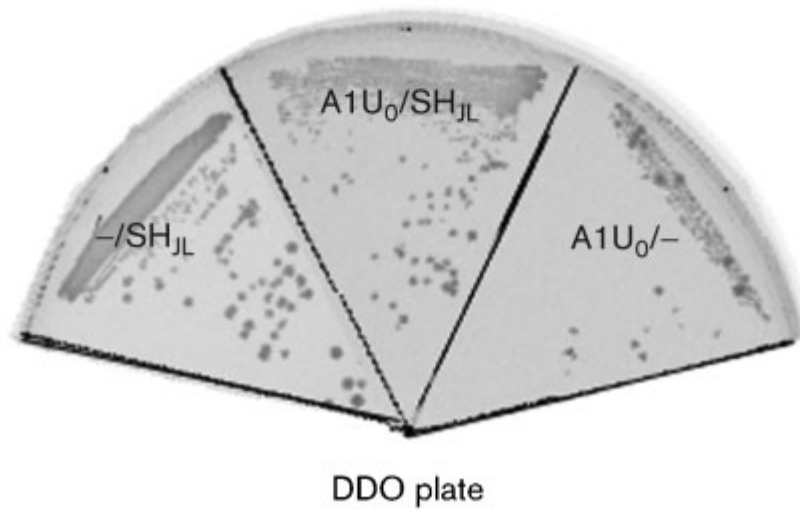
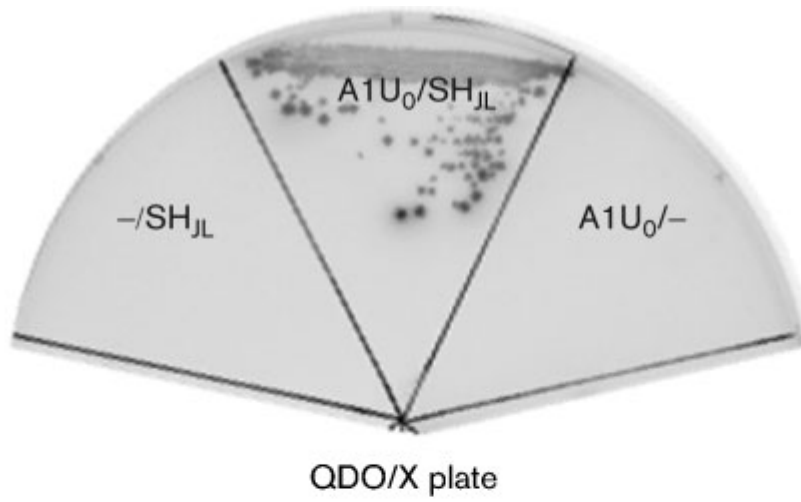
Wilson, R. L., Fuentes, S. M., Wang, P., Taddeo, E. C., Klatt, A., Henderson, A. J. & He, B. (2006). Function of small hydrophobic proteins of paramyxovirus. *J Virol* 80, 1700–1709.

Yates, P. J., Afzal, M. A. & Minor, P. D. (1996). Antigenic and genetic variation of the HN protein of mumps virus strains. *J Gen Virol* 77, 2491–2497.

Figures

Figure 1. (a) Interaction of MuV SH_{JL} and A1U₀ shown in a yeast two-hybrid assay. Yeast strain AH109 was co-transformed with pBD–SH_{JL} and pACT–A1U₀. Interaction of SH_{JL} with the A1U₀ fragment is indicated by growth of colonies on the QDO/X plate (upper panel, middle section). SH_{JL} and A1U₀ showed negative results for autoactivation (upper panel, right and left section). Colonies on DDO plates indicate co-transformation of bait and prey plasmids, respectively (lower panel). (b) Co-immunoprecipitation (co-IP) of A1Up with the SH protein. 293 cells were cotransfected with plasmids pMyc–A1Up and pHA–SH_{wt} (lanes 1 and 2) or pMyc–A1Up and pCMV–HA (lane 3). Cell lysates were subjected to co-IP with rabbit anti-HA antiserum or non-specific rabbit IgG antiserum, as indicated, and protein G–Sepharose. Proteins were separated by SDS-PAGE, then blotted and detected with mouse anti-Myc and anti-HA antibodies. As expression controls for the proteins, the respective cell lysates were immunoblotted using mouse anti-Myc and anti-HA antibodies (lanes 1c, 2c and 3c). Detection of b-actin by a mouse anti-b-actin antibody served as an internal loading control.

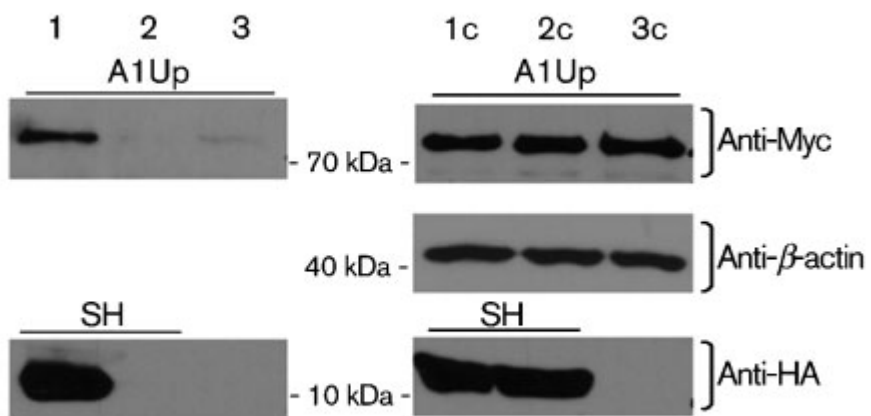
(a)



(b)

Co-immunoprecipitation

Expression control



Anti-HA	+	-	+
Rabbit IgG	-	+	-

Figure 2. Mapping of the interacting domain of A1Up. (a) Map of A1Up. Protein motifs indicated are: UbL, ubiquitin-like domain; UbA, ubiquitin-associated domain; Sti1, stress-inducible heat shock chaperonin-binding motifs; and H, hydrophobic region. Binding activity of the A1Up fragments to SH is summarized to the right. (b) Co-IP of A1Up fragments. 293 cells were co-transfected with pHA-SH_{wt} in combination with pMyc- Δ UbA (1a-1c), pMyc-A1U Δ UbA (2a-2c), pMyc-(3a-3c), pMyc-A1U₁₋₁₄₃ (4a-4c), pMyc-A1U₁₃₆₋₂₇₀ (5a-5c), pMyc-A1U₁₈₆₋₂₇₀ (6a-6c) or pMyc-A1U₂₅₉₋₆₀₁ (7a-7c). Cell lysates were immunoprecipitated with rabbit anti-HA (1a-7a) or non-specific rabbit IgG antiserum (1b-7b) and protein G-Sepharose. Precipitated proteins were analysed by immunoblotting with mouse anti-Myc and anti-HA antibodies (upper panel). Arrowheads indicate the position of precipitated interacting proteins (top right). Ig-LC indicates the immunoglobulin light chain. Protein expression in cell lysates was examined by immunoblotting using Myc- and HA-specific mouse antibodies (1c-7c). Detection of β -actin by a mouse anti- β -actin antibody served as an internal loading control.

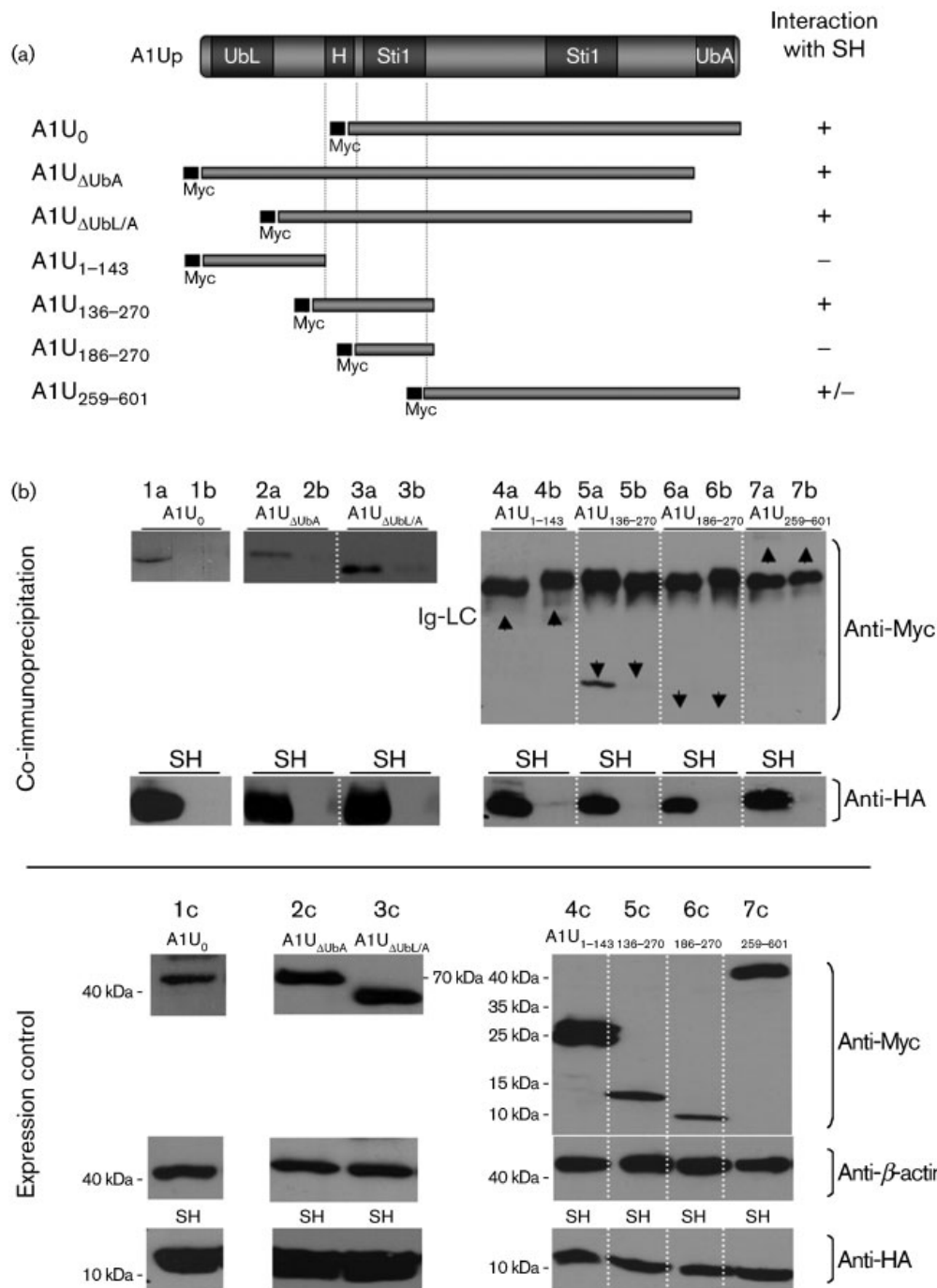


Figure 3. Intracellular distribution of SH and A1Up. Subcellular localization of HA-SH_{wt} and Myc-A1Up was analysed in 293 cells 24 h post-transfection with pHA-SH_{wt} and pMyc-A1Up. Transfected cells were fixed and subjected to immunofluorescence analysis using mouse monoclonal anti-HA, anti-Myc and anti-PDI antibodies as an ER marker and rabbit anti-20S proteasome antiserum, in conjunction with the respective goat anti-mouse or anti-rabbit Fab fragments conjugated with Cy2 (green), Cy3 (red) or Cy5 (white). The smaller sized pictures show a close-up of the rectangular range within the larger image. (a) Solely expressed Myc-A1Up (green) co-stained with 20S proteasome (white) and PDI (red). (b) Solely expressed HA-SH (green) costained with 20S proteasome (white) and PDI (red). (c) Co-expressed Myc-A1Up (red) and HA-SH (green) co-stained with 20S proteasome (white). (d) Co-expressed Myc-A1Up (red) and HA-SH (green) co-stained with PDI (white).

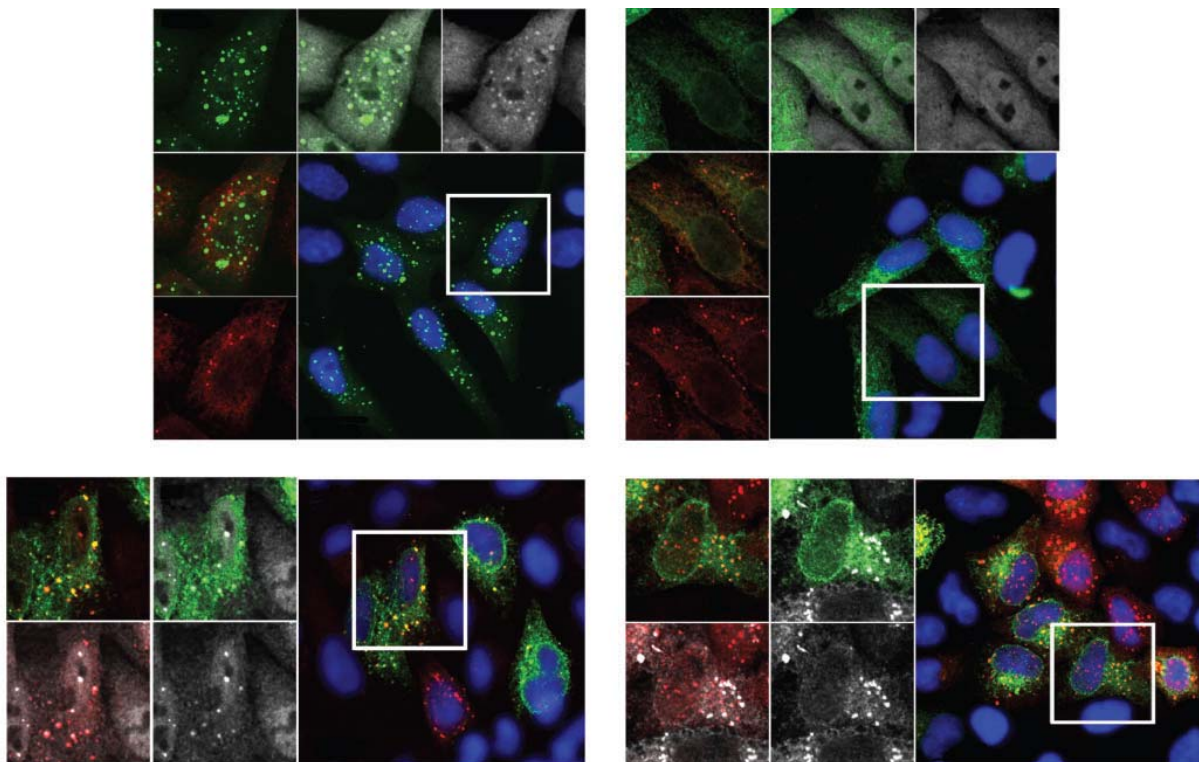


Figure 4. Subcellular localization of SH and A1Up in MuV-infected cells. (a) Vero cells were infected with rMuV EGFP-SH at an m.o.i. of 0.1. Forty-eight hours after infection cells were fixed and stained with anti-PDI antibody in conjunction with an Alexa Fluor 568-conjugated anti-rabbit secondary antibody (Molecular Probes). Pictures were taken by confocal laser scanning microscopy (Leica SP5). (b) Vero cells were infected with rMuV EGFP-SH at an m.o.i. of 0.1 and transfected with pMyc-A1Up. After 48 h, cells were fixed and stained with anti-Myc antibody in conjunction with Alexa Fluor 568-conjugated anti-mouse secondary antibody (Molecular Probes). The lower row shows close-ups of the rectangular range within each of the images above.

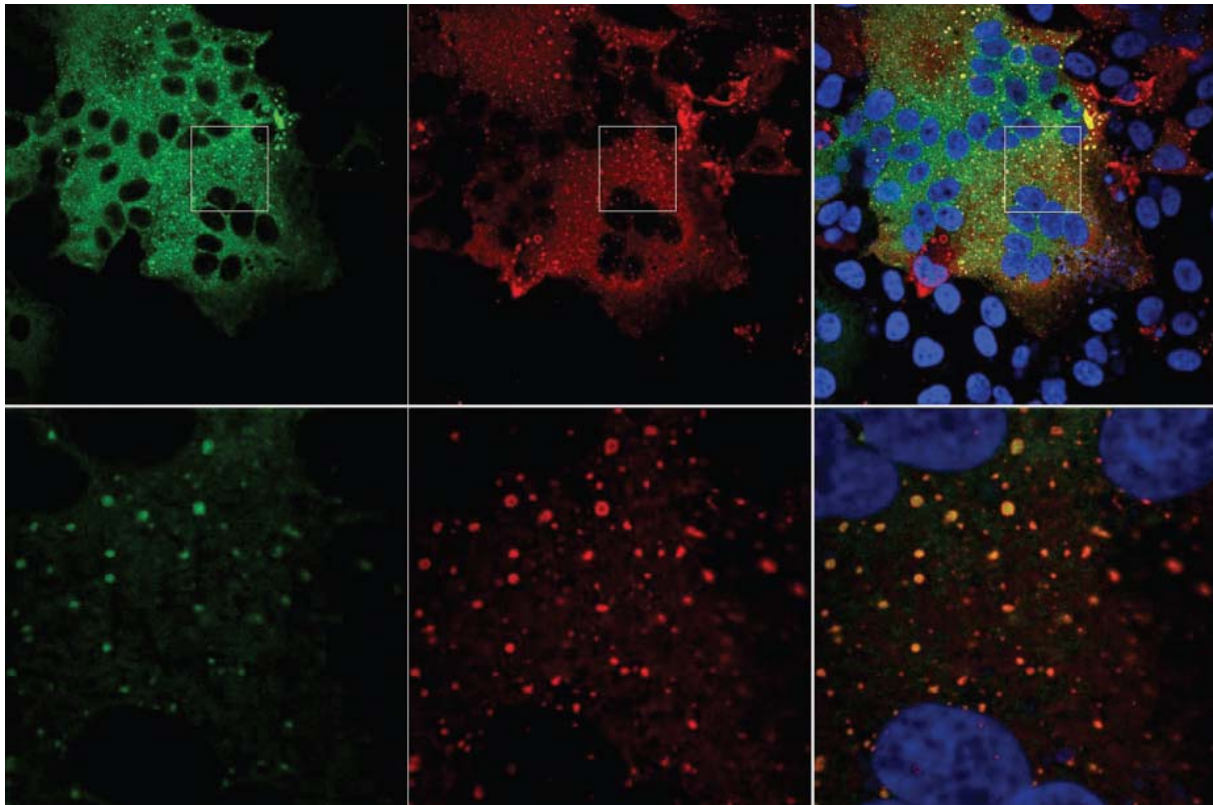


Figure 5. Stability of A1Up and SH. 293 cells were co-transfected with pMyc-A1Up and pHA-SH_{wt}, while pMyc-A1Up/pCMV-HA and pHA-SH/pCMV-Myc were used as negative controls. Fortyeight hours after transfection, cells were incubated with 50 ng cycloheximide ml⁻¹. At 0, 2 and 6 h post treatment, cells were fixed and A1Up and SH protein levels were determined in quadruplicate by indirect ELISA using mouse monoclonal anti- HA and anti-Myc, and peroxidase-conjugated goat anti-mouse antibodies. Circles indicate the degradation of A1Up in the presence (●) and absence (○) of SH. ▲ and Δ indicate the reciprocal experiment for A1Up.

